Performance of Nose Cone Geometries on Sounding Rockets

Nathan Robbins

260774713

McGill University

Abstract

This investigation compares the performances of several nose cone geometries and their suitability for flight on a high-altitude sounding rocket. Many geometries have been proposed to mitigate the extreme aerodynamic forces and phenomena encountered during such high energy ascents. The geometries in question include the conic section, Haack Series nose cone, and the aerospike nose cone; all of which are evaluated according to their coefficients of drag, heating characteristics, and several outstanding factors such as wall shear stress, pressure distributions, and useful internal volume. The investigation concludes that the aerospike nose cone is well suited for high-altitude sounding rockets because of its capacity to reduce drag, its exceptional ability to reduce heating, and its larger useful internal volume. Through this unique combination of performance and volume, the aerospike nose cone is a likely candidate for the forebody of high-altitude sounding rockets for future missions.

Keywords: aerospike nose cone, sounding rocket, Haack Series, conic section, coefficient of drag, aerodynamic heating

Introduction

The upper atmosphere and lower bounds of space remain key areas of interest for scientific study and the advancement of technology. Accessing these areas consistently and rapidly, however, has proven to be a difficult task. High-altitude sounding rockets deliver the exact precision and speed required to study areas such as the upper atmosphere and near-Earth space. Difficulties arise when considering the immense aerodynamic pressures, drag, and heating to which this rapid ascent subjects the vehicle. The nature of the high-altitude sounding rocket's ascent requires it to accelerate from rest to supersonic speeds within a matter of seconds. Thus, the airframe experiences subsonic, transonic, supersonic, and occasionally hypersonic speeds over the course of its flight. As the flight conditions change, so do the geometries that optimize performance, so determining the ideal nose cone geometry for all three regimes of flight becomes a complex task. A variety of aerodynamic surfaces have traditionally been used to combat drag and heating, each with its own set of advantages and disadvantages in each regime of flight. Finding a suitable nose cone for flight is imperative to the viability and success of a mission.

This paper seeks to compare classic geometries such as conics and Haack Series to the aerospike nose cone, evaluating their performances on the typical ascent profile of a sounding rocket. The aerodynamic effects of drag and heating will be considered in great detail, as well as other factors such as volume and shear stress. All things considered, the blunt-body aerospike nose cone shows great potential as a replacement for more classical nose cone geometries previously used for high-altitude sounding rockets. This is because of its moderate effect on drag at supersonic speeds, its ability to reduce heating, and its increased internal volume.

Background

A typical sounding rocket launched for scientific purposes will have a target altitude between one hundred kilometers and five hundred kilometers. This paper will take the Black Brant IX as an example of a typical flight, with the data from *Table 1* serving as the basis for what is considered typical. As seen in *Table 1*, the vehicle reaches an altitude of three kilometers within six seconds, implying an average velocity of 0.5 kilometers per second, or Mach 1.5, showing how quickly the vehicle exits both the subsonic and transonic regimes of flight. From this point onward, the vehicle travels at supersonic and hypersonic speeds upwards of Mach 7, eventually reaching an apogee of 330 kilometers (Christie et al., 2016). Due to the brief time spent subsonic and transonic, emphasis will be placed on nose cone performances at supersonic and hypersonic speeds.

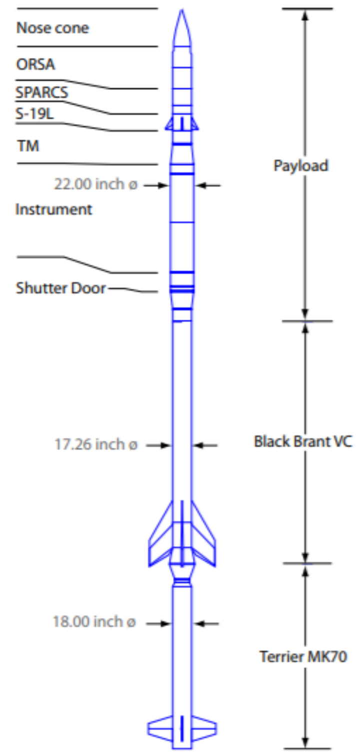

Figure 1: Terrier-Black Brant IX flight configuration (Christie, Zeiger, Pfaff, & Garcia, 2016)

Event	Time (s)	Altitude (km)
Motor Ignition	0	0
Terrier Burnout	6	3
Black Brant Ignition	12	6
Black Brant Burnout	46	50
Despin	60	80
Payload Separation	64	88
SPARCS/CACS Enable	66	93
Shutter Door Open	67	95
Observations Begin	110	180
Apogee	300	330
Shutter Door Closes		
Observations End	500	140
Parachute Deploy	690	2
Payload Impact	1000	0

Table 1: Terrier-Black Brant IX flight profile (Christie et al., 2016)

The simplest of nose cone shapes is the conical body of revolution. *Figure 2* displays the conical geometry, while *Figure 3* illustrates different forms of the Haack Series nose cone. While not often used, due to its smaller internal volume, structurally weak tip, and sub-optimal drag, the conic section will be used as a baseline to compare the performances of other nose cone geometries (Chin, 1961).

Figure 2: The conical body of revolution (Chin, 1961)

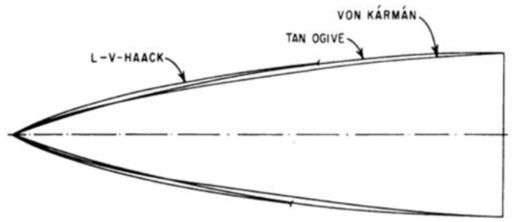

Figure 3: Various Haack Series geometries (Chin, 1961)

The Haack Series nose cones are "derived theoretically from aerodynamic drag consideration" (Chin, 1961, p. 27) and give various optimizations for given parameters, including length, diameter, and volume. Perhaps the most well-known Haack Series nose cone is the Von Karman nose cone, which is derived to minimize drag for a given length and diameter. The equation defining Haack Series cones is shown below:

$$r = \frac{1}{\sqrt{\pi}}\sqrt{\varphi - \frac{1}{2}\sin 2\varphi C \sin 3\varphi} \qquad \text{(Chin, 1961)}$$

Where: $\varphi = \cos^{-1}(1 - 2x)$ and C = 0 for the Von Karman and 1/3 for the L-V Haack Series.

The aerospike nose cone deviates significantly from the aforementioned nose cones in that it is notably blunt shaped and has a rod protruding forward. This counter-intuitive design results in a complex sequence of aerodynamic phenomena. As depicted in *Figure 4*, in both supersonic and hypersonic airflow, the aerospike produces a bow shock about its blunt end, resulting in flow separation and recirculation zones within this bow shock. The recirculation zone, located just before

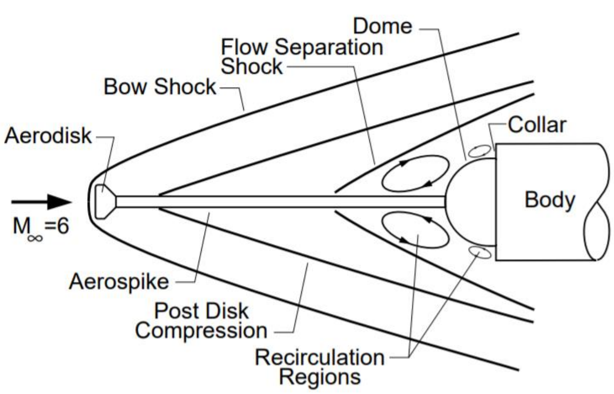

Figure 4: Hypersonic flow over a typical aerospike (Huebner, Mitchell, & Boudreaux,1995)

the main body, "effectively reduces the pressure and heating distributions on the hemispherical dome and also allows them to be more uniform" (Huebner et al.,1995, p. 2). This phenomenon has clear implications for flight; however, it relies on the appearance of shockwaves and is therefore only practical when considering transonic, supersonic, and hypersonic flow.

Analysis

In order to evaluate the performance of each nose cone, three principal criteria are examined. First, the coefficient of drag is analysed to determine which geometry is most aerodynamically efficient. Following this, the heating characteristics are studied as they pertain to the structural integrity of the forebody and internal components. Finally, various factors such as shear stress, the distribution of pressure, and internal volume are compared to gain a comprehensive understanding of each geometry's performance on a sounding rocket. The synthesis of these criteria shows the desirable effects of the aerospike nose cone as compared to traditional geometries.

Coefficient of drag

The coefficient of drag of the forebody of a sounding rocket is perhaps the most important criterion to consider for flight. Ultimately, the coefficient of drag will determine the maximum altitude that the vehicle is capable of reaching, for a given weight, thrust, and rate of fuel consumption. The conical body of revolution is a classic example of the forebody of a sounding rocket. While simple in shape and manufacture, the conic section has serious disadvantages when compared to other geometries. A conic section of half angle 9 ˚ has a free-molecule coefficient of drag of 2.34 when subject to an airspeed of Mach 6 (Wendt, 1972). The Haack Series nose cone, however, has a lower foredrag coefficient when compared to most other geometries, as is shown in Appendix A (Perkins, Jorgensen, & Sommer, 1952). While the foredrag coefficient is not directly comparable to the coefficient of drag, Appendix A gives a good estimation for the comparative performances of the various geometries. By contrast, when considering the aerospike nose cone at Mach 5.75, *Figure 5* shows that this geometry can have a coefficient of drag less than 1.0. Moreover, at lower Mach speeds, blunt-body aerospikes can reduce the coefficient of drag by up to 68% (Sahoo, Das, Kumar, & Parasad, 2016); a result which is further supported by Huang, Li, Yang, and Zhang (2017). These results demonstrate that, although not the most effective aerodynamically, the aerospike nose cone remains an efficient method of reducing the drag of a high-altitude sounding rocket.

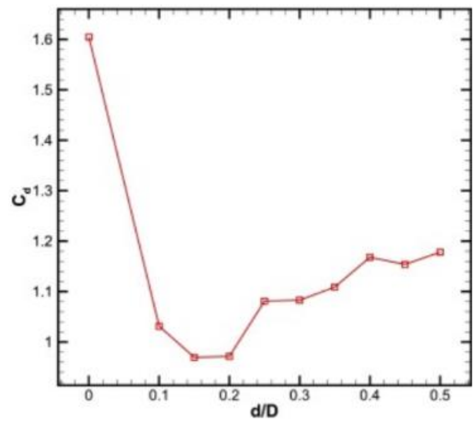

Figure 5: Coefficient of drag and disk-to-body diameter ratio for an aerospike (Chinnappan, Malaikannan, & Kumar, 2017)

Heating characteristics

One of the most prominent consequences of high-speed air travel is the aerodynamic heating of the launch vehicle. Intense and continued heating can cause the unplanned failure of components and ultimately the failure of the entire launch vehicle. For a conic section, as shown in *Figure 6*, the surface temperature along the cone remains notably higher for a prolonged distance along the surface (Amini, Emdad, Akramian, & Bordbar, 2012).

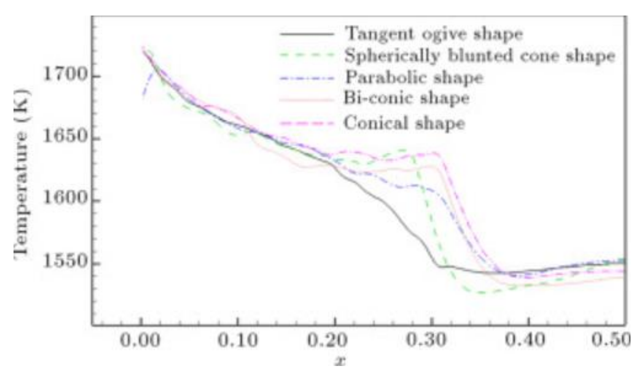

Figure 6: Surface temperature at Mach 5 for various geometries (Amini et al., 2012)

Amini et al. (2012) found that most geometries have surface temperatures that steadily decrease away from the tip; however, the cone's surface temperature begins above 1700K, decreases to approximately 1650K, then maintains this temperature until reaching the end of the cone at a lateral distance of 0.3m from the tip. While the exact heating characteristics of the Haack Series were not found, the surface temperature likely follows a similar distribution to those shown in *Figure 6*, as they all share similar underlying geometries. When considering an aerospike, however, it has been shown that there "is truly […] an advantage in terms of pressure and thermal loading reductions on the dome at [an angle of attack of] α=0" (Huebner et al., 1995, p. 5). Nevertheless, Huebner et al. (1995) also found that this advantage rapidly disappears as the angle of attack increases (refer to Appendix B). Additionally, a small forebody diameter on an aerospike nose cone can result in an increased heat flux at the main body (Chinnappan et al., 2017); an outcome which endangers the integrity of the launch vehicle. Despite these effects, the aerospike nose cone outperforms the other geometries with its superior ability to reduce thermal loading on the forebody of the vehicle.

Miscellaneous factors

While the coefficient of drag and the heating effects of a high-altitude sounding rocket are of extreme importance to the success of the mission, there are many other factors which cannot be easily categorized, yet remain of critical importance. One such factor is the appearance of shockwaves over the cone. Yanamashetti, Suryanarayana, and Mukherjee (2017) found that the appearance of shockwaves on a 20˚ conic nose in transonic flow is identified before the appearance of shockwaves on an ogive nose cone. While this study considers an ogive cone and not a Haack Series, the same principle applies that the sharp vertices of the cone induce shockwaves (Yanamashetti et al., 2017). Furthermore, the wall shear stress on a conic section is steady and elevated relative to that of other geometries (Amini et al., 2012). These two results imply that the cone, while simple, is an unfavourable geometry as the stresses and aerodynamic shocks on the forebody appear earlier and in more intensity than geometries such as the ogive or Haack Series. The aerospike, however, exhibits a decreasing static pressure along its surface as the length of the spike is increased (Huang et al., 2017); showing that there is an advantage to having the aerospike extend into the oncoming flow as opposed to not having it. A final, yet significant, criterion to consider is the useful internal volume that these geometries allow. Approaching the tip of the cone, both conic sections and Haack Series cones become quite small in cross section. Comparatively, the aerospike allows for a large dome-like forebody, thus maximizing the available useful space for internal systems. These various factors show the advantage to having an aerospike nose cone as opposed to the conic section or Haack Series nose cones on high-altitude sounding rockets.

Parameter	A0	A1	A2	A3
L(mm)	40	40	40	40
D(mm)	0	10	14	18

Table 2: Lengths and diameters of aerodisks used in *Figure 7* (Huang et al., 2017)

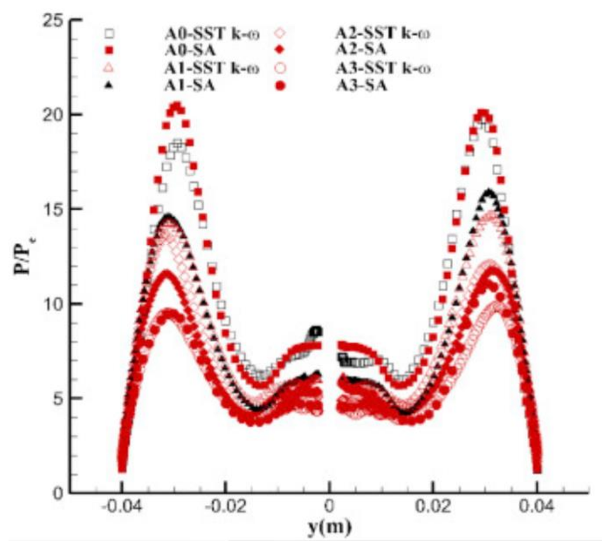

Figure 7: Static pressure along the surface of an aerospiked dome (Huang et al., 2017)

Conclusion

The aerospike nose cone proves to be a fitting alternative to traditional sounding rocket nose cones such as the conic section and Haack Series cones. When considering the coefficient of drag, the Haack Series and aerospike show exceptional performance at supersonic speeds.

Nevertheless, the heating characteristics of the aerospike nose cone surpass those of the other geometries, as the induced bow shock produces ideal flow conditions over the dome of the vehicle. Moreover, the useful internal volume of the aerospike nose cone has the potential to be much greater than that of its counterparts. Accordingly, the aerospike nose cone is well suited for the performance of high-altitude sounding rockets. As the demand for easy access to the upper atmosphere and space grows, the aerospike looks to be a forerunner in launch vehicle technologies.

References

Amini, Y., Emdad, H., Akramian, K., & Bordbar, F. (2012). Investigation of the common nose cone shapes in different gas mixtures in high Knudsen numbers. *Scientia Iranica, 19*(6), 1511-1518. https://doi.org/10.1016/j.scient.2012.10.029

Chin, S.S. (1961). *Missile Configuration Design*. Retrieved from https://babel.hathitrust.org/cgi/pt?id=mdp.39015015426904;view=1up;seq=7

Chinnappan, A.K., Malaikannan, G., & Kumar, R. (2017). Insights into flow and heat transfer aspects of hypersonic rarefied flow over a blunt body with aerospike using direct simulation Monte-Carlo approach. *Aerospace Science and Technology, 66*, 119-128. https://doi.org/10.1016/j.ast.2017.02.024

Christe, S., Zeiger, B., Pfaff, R., Garcia, M. (2016). Introduction to the Special Issue on Sounding Rockets and Instrumentation. *Journal of Astronomical Instrumentation, 5*. https://doi.org/10.1142/S2251171716020013

Huang, W., Li, L.-q., Yan, L., & Zhang, T.-t. (2017). Drag and heat flux reduction mechanism of blunted cone with aerodisks. *Acta Astronautica, 138,* 168-175. doi:10.1016/j.actaastro.2017.05.040

Huebner, L.D., Mitchell, A.M., & Boudreaux, E.J. (1995). *Experimental results on the feasibility of an aerospike for hypersonic missiles.* Washington: American Institute of Aeronautics and Astronautics. Retrieved from: https://www.cs.odu.edu/~mln/ltrs-pdfs/aiaa-95-0737.pdf

Perkins, E.W., Jorgensen, L.H., & Sommer, S.C. (1952). *Report 1386: Investigation of the drag of various axially symmetric nose shapes o fineness ratio 3 for mach numbers from 1.24 to 7.4.* California: National Advisory Committee for Aeronautics, Ames Aeronautical Laboratory. Retrieved from: http://naca.central.cranfield.ac.uk/reports/1958/naca-report-1386.pdf

Sahoo, D., Das, S., Kumar, P., & Parasad, J.K. (2016). Effect of spike on steady and unsteady flow over a blunt body at supersonic speed. *Acta Astronautica, 128,* 521-533. https://doi.org/10.1016/j.actaastro.2016.08.005

Wendt, J.F. (1972). *Drag coefficient of cones*. Rhode Saint Genese: Air Force Flight Dynamics Laboratory, von Karman Institute for Fluid Dynamics. Retrieved from http://www.dtic.mil/dtic/tr/fulltext/u2/750042.pdf/

Yanamashetti, G., Suryanarayana, G. K., & Mukherjee, R. (2017). Development of Flow over Blunt-Nosed Slender Bodies at Transonic Mach Numbers. Paper presented at the 15th Asian Congress of Fluid Mechanics, ACFM 2016, November 21, 2016 - November 23, 2016, Kuching, Sarawak, Malaysia.

Appendix A

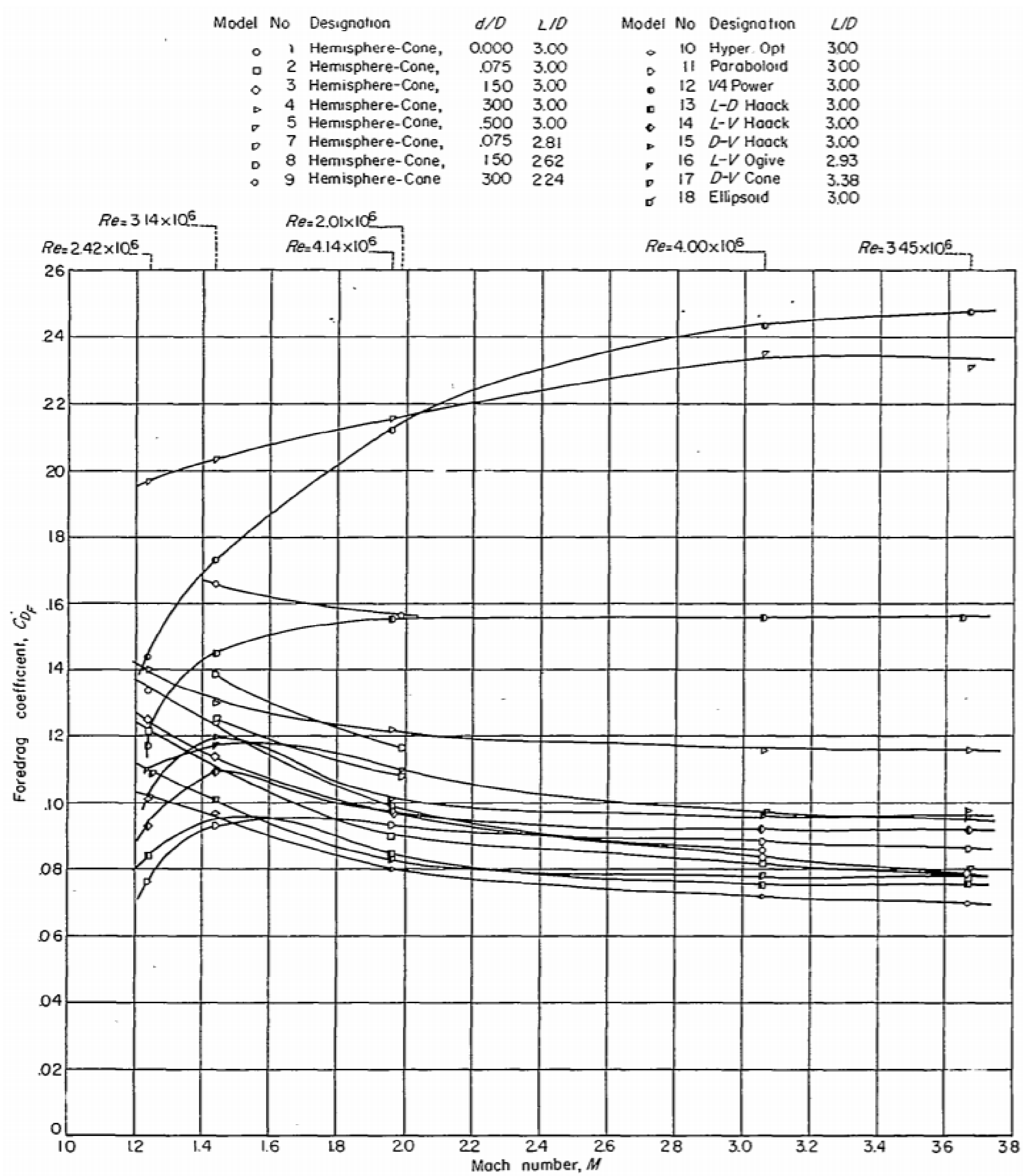

Figure A1: Variation in foredrag coefficient with Mach number for different nose cones (Perkins, Jorgensen, & Sommer, 1952)

Appendix B

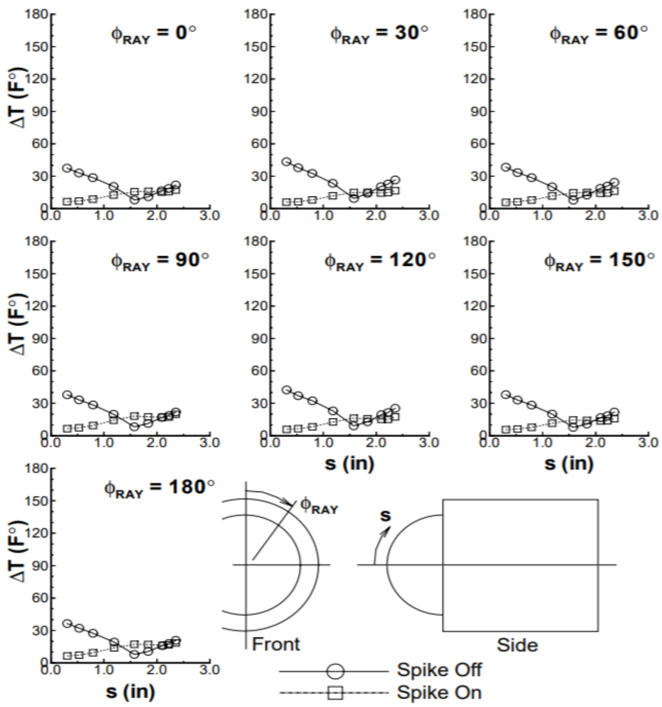

Figure B1: Surface temperature rise on the dome of an aerospiked cone at an angle of attack of 0˚ (Huebner et al.,1995)

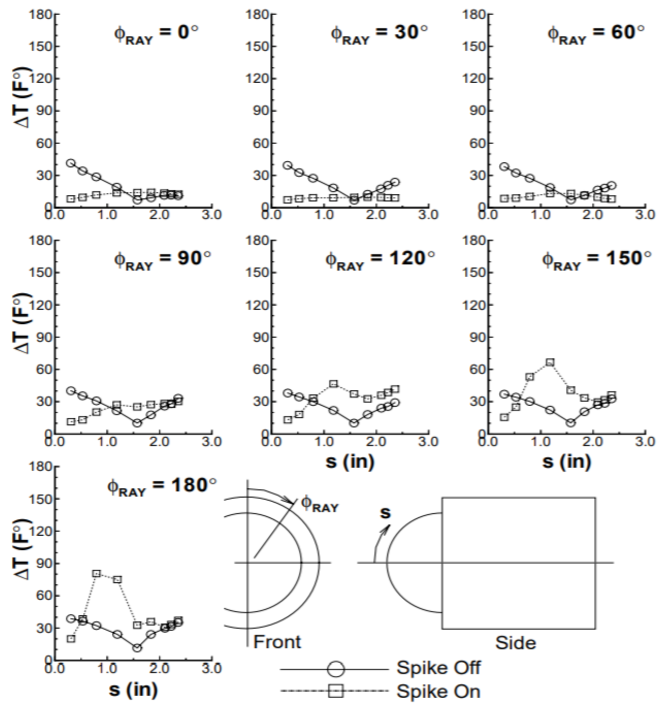

Figure B2: Surface temperature rise on the dome of an aerospikes cone at an angle of attack of 5˚ (Huebner et al.,1995)